Bioorganic & Medicinal Chemistry Letters xxx (2015) xxx–xxx

Contents lists available at ScienceDirect

Bioorganic & Medicinal Chemistry Letters

journal homepage: www.elsevier.com/locate/bmcl

# Selective inhibition of PARP10 using a chemical genetics strategy

Rory K. Morgan, Ian Carter-O'Connell, Michael S. Cohen *

*Program in Chemical Biology and Department of Physiology and Pharmacology, Oregon Health & Science University, 3181 SW Sam Jackson Park Rd, #L334, Biomedical Research Building, Rm 621, Portland, OR 97239-3098, United States*

ARTICLE INFO

*Article history:*
Received 4 May 2015
Revised 10 July 2015
Accepted 13 July 2015
Available online xxxx

*Keywords:*
PARPs
Chemical genetics
ADP-ribosylation
Click chemistry

ABSTRACT

The lack of inhibitors that are selective for individual poly-ADP-ribose polymerase (PARP) family members has limited our understanding of their roles in cells. Here, we describe a chemical genetics approach for generating selective inhibitors of an engineered variant of PARP10. We synthesized a series of C-7 substituted 3,4-dihydroisoquinolin-1(2*H*)-one (dq) analogues designed to selectively inhibit a mutant of PARP10 (LG-PARP10) that contains a unique pocket in its active site. A dq analogue containing a bromo at the C-7 position demonstrated a 10-fold selectivity for LG-PARP10 compared to its WT counterpart. This study provides a platform for the development of selective inhibitors of individual PARP family members that will be useful for decoding their cellular functions.



Poly-ADP-ribose polymerases (PARPs) are a family of 17 ubiquitously expressed enzymes in humans that catalyze the transfer of the ADP-ribose moiety from nicotinamide adenine dinucleotide ($NAD^+$) to their target proteins, a process known as ADP-ribosylation (ADPr). Only four PARPs catalyze poly-ADPr (PARP1, **2**, **5a**, and **5b**), whereas the majority of the PARPs catalyze mono-ADPr.[1] PARPs are found throughout the cell and play roles in diverse cellular processes, including transcriptional[2] and post-transcriptional regulation,[3] protein degradation,[4] cell signaling[5,6] and the unfolded protein response.[7] However, the cellular functions and targets of most PARPs—especially those that catalyze mono-ADPr—remain unknown and current strategies to study PARP function are insufficient to provide a comprehensive view of their role in cellular processes. This is due, in large part, to the dearth of inhibitors that selectively inhibit an individual PARP family member.

A major hurdle for developing selective PARP inhibitors is the high structural conservation of the catalytic domain among PARPs. While the primary sequences are semi-divergent (displaying ~50% similarity),[8] their structures are highly conserved in the nicotinamide-binding site, which is the major binding site for the majority of PARP inhibitors.[9] To address this challenge, we implemented a chemical genetics strategy, commonly referred to as the 'bump-hole' method, for the development of selective PARP inhibitors. This strategy has been successfully used for identifying highly selective inhibitors of an individual enzyme within a highly conserved family,[10] most notably protein kinases.[11] In this Letter, we describe a bump-hole approach for identifying selective inhibitors of individual PARPs.

We recently described a bump-hole method for identifying the direct protein targets of PARPs that catalyze poly-ADPr.[12] This method involved mutating a lysine residue (Lys903 in human PARP1, which we refer to as the 'ceiling' position) in the nicotinamide-binding site to an alanine to create a unique pocket for accommodating a C-5 ethyl group on the nicotinamide ring of the $NAD^+$ analogue. We sought to adopt this chemical genetics strategy to generate selective inhibitors of PARP10. We focused our initial efforts on PARP10 since its mono-ADPr activity has been well characterized in vitro.[13] While inhibitors of PARP10 have been previously reported, they are not selective among the PARP family.[14]

We first examined the crystal structure of PARP10 bound to the nicotinamide bioisostere 3-aminobenzamide (3-AB) (PDB ID: 3HKV) to identify potential inhibitor-sensitizing positions within the nicotinamide binding site (Fig. 1a). We focused on Leu926 (human PARP10 numbering) because it occupies the same space in the nicotinamide-binding pocket as the ceiling lysine of PARP1. We reasoned that mutation of Leu926 to either an alanine or glycine would create a unique pocket for orthogonal inhibitors. We first determined if mutation of Leu926 to an alanine or glycine (LA-PARP10 or LG-PARP10, respectively) affects the activity of the catalytic domain of PARP10 ($PARP10_{cat}$). To test the activity of LA-, LG-, and WT-$PARP10_{cat}$ we monitored ADP-ribosylation of SRSF protein kinase 2 (SRPK2), a previously characterized PARP10 substrate,[15,16] using *N*-6 alkyne-$NAD^+$ (6-a-$NAD^+$)[12,17] and click conjugation to a fluorescent azide reporter (Fig. 1b). Using this

* Corresponding author. Tel.: +1 503 418 1363.
*E-mail address:* cohenmic@ohsu.edu (M.S. Cohen).

http://dx.doi.org/10.1016/j.bmcl.2015.07.033
0960-894X/

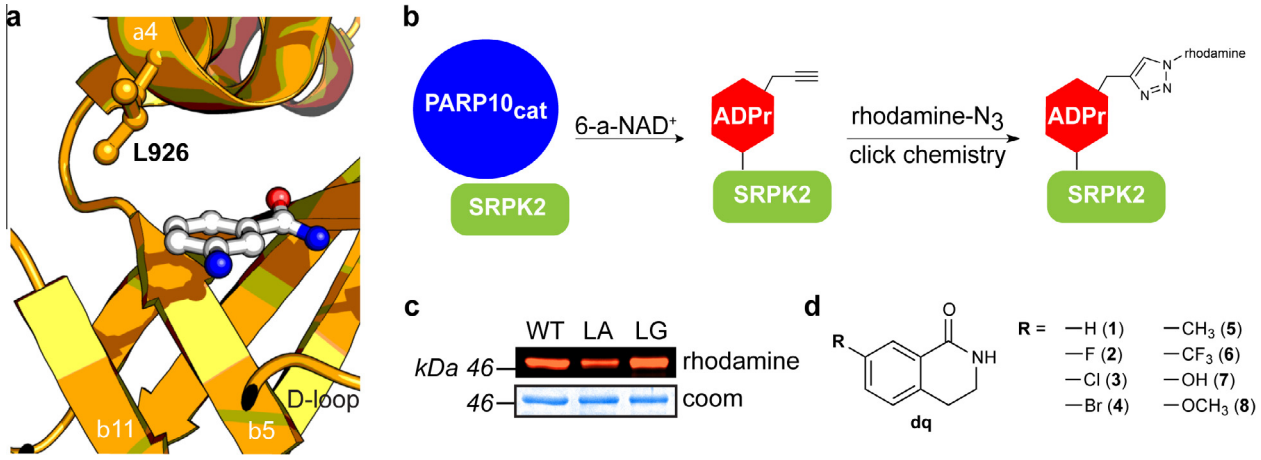


**Figure 1.** A chemical genetics strategy for generating selective inhibitors of PARP10. (a) Structure of PARP10 with nicotinamide isostere 3-aminobenzamide (3-AB) (PDB ID: 3HKV) with mutated residue (L926) indicated. (b) Schematic showing the PARP10-mediated transfer of alkyne-tagged ADP-ribose onto SRPK2 from 6-a-NAD$^+$, followed by click conjugation with a fluorescent azide reporter (rhodamine-$N_3$). (c) Activity comparison of engineered PARP10$_{cat}$ mutants L926A (LA) and L926G (LG) to WT-PARP10$_{cat}$. (d) Structure of C-7 substituted dq analogues **1**–**8** designed to selectively inhibit engineered PARP10 mutants.

assay, we found that both engineered PARP10$_{cat}$ mutants exhibited similar activity to WT-PARP10$_{cat}$ (Fig. 1c). A more detailed analysis using a range of 6-a-NAD$^+$ concentrations revealed that LG-PARP10$_{cat}$ exhibited ~60% activity of WT-PARP10$_{cat}$ (Fig. S1).

We next sought to identify compounds that could selectively inhibit our engineered PARP10 mutants. As a starting point for our inhibitor design, we selected 3,4-dihydroisoquinolin-1(2*H*)-one (dq, **1**), a pan-PARP inhibitor scaffold that binds in the same orientation as 3-AB in the nicotinamide binding site.[18] We designed a series of dq analogues containing various substituents at the C-7 position to probe the size and shape of the unique pocket in our engineered PARP10 mutants (Fig. 1d). We used two different strategies to synthesize C-7 dq analogues. Analogues **3**–**8** were synthesized using the Schmidt reaction (Scheme 1). The reaction resulted in a mixture of both *N*-alkyl and *N*-aryl regioisomers, which were easily resolved with standard normal phase chromatography. The percentage of the desired *N*-alkyl isomer obtained from the Schmidt reaction ranged from 26% to 63% (Supporting information). The yield of the *N*-alkyl isomer was highest for 1-indanones where the 6-position substituent was highly electron donating (e.g., –OH, –$OCH_3$), whereas *N*-alkyl regioselectivity decreased with electron withdrawing substituents (e.g., –Cl, –Br, –$CF_3$). The fluoro-substituted dq derivative **2** was synthesized via a previously described route that involves the formation of the methylcarbamate species from *p*-fluorophenethylamine followed by intramolecular cyclization in triflic acid (Scheme 2 and Supporting information).[19]

We first tested our panel of C-7 substituted dq analogues against our engineered PARP10$_{cat}$ mutants. In a preliminary screen, we found that none of the compounds inhibited the LA-PARP10$_{cat}$ mutant (data not shown); therefore, we focused on LG-PARP10$_{cat}$. We found that most of the C-7 substituted dq analogues inhibited LG-PARP10$_{cat}$ more potently than the parent dq scaffold **1** (Fig. 2a and b, Table 1, and Fig. S2). A clear structure-activity relationship is observed for the halogen series: increasing the size of the halogen group resulted in increased potency against LG-PARP10$_{cat}$, with the bromo-substituted dq analogue **4**

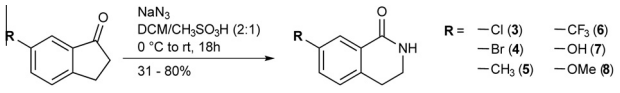


**Scheme 1.** Syntheses of analogues **3**–**8** via Schmidt reaction.

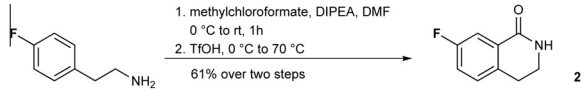


**Scheme 2.** Synthesis of analogue **2** via intramolecular aromatic substitution reaction.

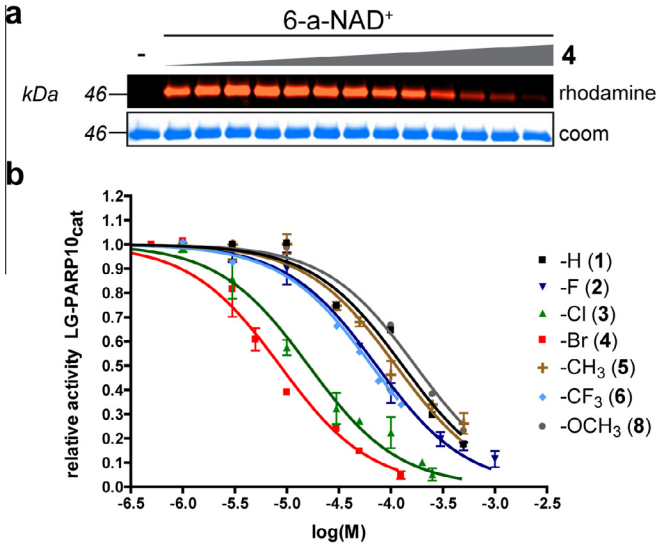


**Figure 2.** C-7 substituted dq analogues selectively inhibit LG-PARP10$_{cat}$. (a) Representative fluorescent gel image showing a dose-dependent inhibition of LG-PARP10$_{cat}$-mediated ADP-ribosylation of SRPK2 by 7-Br-dq (**4**). SRPK2 (3 μM) was ADP-ribosylated by LG-PARP10$_{cat}$ (500 nM) with 6-a-NAD$^+$ (100 μM) in the presence of analogue **4** (0–125 μM) at 30 °C for 1 h. Following click conjugation to rhodamine-azide (100 μM), proteins were resolved by SDS–PAGE and detected via in-gel fluorescence. Coomassie (Coom) Brilliant Blue staining was used to demonstrate even loading. (b) $IC_{50}$ curves for C7-substituted dq analogues against LG-PARP10$_{cat}$. Activity was determined as described in (a). Error bars represent SEM, $n = 2$.

exhibiting the greatest potency ($IC_{50}$ = 8.6 μM; Fig. 2a and b, Table 1, and Fig. S2). Unlike the halogen-substituted analogues, the methyl (**5**), methoxy (**8**), and hydroxyl (**7**) dq analogues did not exhibit increased potency compared to **1** (Fig. 2b, Table 1, and Fig. S2). The trifluoromethyl dq analogue **6** exhibited a modest, 2-fold increase in potency compared to **1** (Fig. 2b, Table 1, and